ORIGINAL ARTICLE

Kinetic and isotherm modeling for acid blue 113 dye adsorption onto low-cost nutraceutical industrial fenugreek seed spent

Mohammed A. H. Dhaif-Allah[1,2] · Syed Noeman Taqui[3] · Usman Taqui Syed[4] · Akheel Ahmed Syed[5]

Abstract

The present study reports about the use of fenugreek seed spent as a new and efficient biosorbent for the removal of acid blue 113 dye from aqueous media and textile industrial effluent. The spent is a low-cost by-product of nutraceutical industry. The effects of various process parameters of adsorption, such as pH, initial dye concentration, adsorbent dose, adsorbent particle size, contact time and temperature onto nutraceutical industrial fenugreek seed spent (NIFGS) have been studied. Four numbers of two-parameter and six numbers of three-parameter isotherm models were used in the analysis of adsorption equilibrium data. Kinetic studies data conformed to pseudo-second-order model. Molecular diffusion studies were carried out using Weber–Morris, Dumwald–Wagner and film diffusion models. Change in enthalpy ($\Delta H°$), entropy change ($\Delta S°$) and Gibbs free energy change ($\Delta G°$) of adsorption system indicated that the process is physisorption. Scanning electron microscopy, Fourier transform infrared spectroscopy and point of zero charge were used in characterizing the adsorbent. Fractional factorial experimental design and analysis of variance along with statistically developed model for adsorption helped to predict for a maximum adsorption of 661.5 mg g^{-1} using NIFGS. Application of NIFGS to textile industrial effluent and scaling up of the experimental process by three orders gave encouraging results.

Keywords Acid blue 113 · Adsorption isotherm · ANOVA · Kinetics · Nutraceutical industrial fenugreek seed spent

List of symbols

R^2	Correlation coefficient
χ^2	Chi-squared test
C_o	Initial concentration (μg ml^{-1})
C_e	Equilibrium concentration (μg ml^{-1})
q_e	Adsorption capacity (mg g^{-1})
Q_m	Maximum adsorption capacity (mg g^{-1})
q_t	Adsorption capacity at time 't' (mg g^{-1})
$\Delta G°$	Standard free energy
$\Delta S°$	Entropy change
$\Delta H°$	Enthalpy change
R_L	Separation factor
n_F	Heterogeneity factor

Abbreviations

NIS	Nutraceutical Industrial Spent
NIFGS	Nutraceutical Industrial Fenugreek Spent
AB113	Acid blue 113
FTIR	Fourier transform infrared spectroscopy
SEM	Scanning electron microscopy
SSE	Sum of square errors

✉ Akheel Ahmed Syed
akheelahmed54@gmail.com

1 Department of Studies in Environmental Science, University of Mysore, Manasa Gangothri, Mysuru 570006, India

2 Department of Agriculture, Faculty of Agriculture and Veterinary Medicine, Thamar University, Dhamar, Republic of Yemen

3 Department of Chemistry, University of Malaya, 50603 Kuala Lumpur, Malaysia

4 LAQV-REQUIMTE, Department of Chemistry, Faculty of Science and Technology, Universidade NOVA de Lisboa, 2829-516 Caparica, Portugal

5 Department of Studies in Chemistry, University of Mysore, Manasa Gangothri, Mysuru 570006, India

Introduction

It is of utmost importance as also of societal concern about the large-scale depletion of natural resources as also the environmental regulations which have diverted the attention of people in search for getting clean air, soil and water. In textile industry, it is of great concern to reduce the consumption of water as also reducing carbon footprint (Zaffalon 2010). The current value of textile industry which placed at

around US$ 120 billion is likely to reach US$ 230 billion in 2020. This industry, in its magnitude, is next only to agriculture in employing man power engaging over 45 million people directly and 20 million people indirectly. Textile industry contributes 2 percent to India's gross domestic product and 14 percent to overall index of industrial production. There are two sectors which are operating in textile industry. The first one is the organized sector which comprises spinning; apparel and garments use modern machinery and techniques. As against this, the second is the unorganized sector comprising handloom, handicrafts and sericulture which usually operate on small scale and use only traditional tools and methods (www.ibef.org). Between these, the latter uses old machineries, adopts out-dated technologies and uses variety of synthetic dyes ultimately leading to environmental or more precisely water pollution.

Azo dyes constituting the largest class of synthetic dyes are integral part of textile industry and make up to about 70% of commercial dyes (Hubbe et al. 2011). They are extensively used for dyeing cloths and are used at 60 °C, while majority of other dyes need boiling temperature. These dyes are valued much since they offer wide range of colors, provide extreme color fastness and the intensity of color is much more than any nearest alternative, thereby making them invaluable to the textile industry (Carliell et al. 1998). Azo dyes are characterized by structures with one or more azo group (–N=N–) that are bound to the aromatic rings having recalcitrant molecular structure. Under certain circumstances, the azo groups are subject to cleave producing potentially harmful aromatic amines (de Lima et al. 2007). Hence, the removal of these dyes from wastewater by any usual biological, chemical and physical methods is of paramount importance. Although several methods have been reported, they are having such limitations as high cost of plant and machinery, non-affordable operational costs, regeneration, secondary pollutants, sensitivity toward waste water contents, interference by extraneous waste water constituents and residual sludge generation (Szyguła et al. 2008; Dávila-Jiménez et al. 2005).

Acid blue 113 (AB113) is categorized as bis-azo dye which is extensively used for dyeing wool, silk and polyamide fibers from a neutral or acid bath to obtain deep shade of navy blue color (Green 1990). There is limited information reported about its decoloration, degradation and/or adsorption from water. Based on the techniques, methods and procedures reported, these could be classified into six broad categories which include biological-cum-chemical (Eskandarian et al. 2014; Lee et al. 2015; Khehra et al. 2005; Srinivasan and Mishra 2008; Husain et al. 2010), electrocoagulation (Saravanan et al. 2010), physical methods using UV radiation (Shu et al. 2015, 2016a, b; Shu et al. 2005; Rai et al. 2013), photocatalytic degradation (Thejaswini and Prabhakaran 2016; Zayani et al. 2008), low frequency ultrasound-assisted degradation (Sathishkumar et al. 2014), nanomaterials (Shu et al. 2016c) and use of inorganic materials including activated carbons (Gupta et al. 2011; Shu et al. 2010; Shirzad-Siboni et al. 2014; Pura and Atun 2009; Shokohi et al. 2011; Talwar et al. 2016). Reports are lacking on the application of agro-based biological materials for the remediation of AB113 from water.

The growing demand for nutraceuticals across the world as alternative to allopath or modern systems of medicine has attracted the attention of many industries including the pharmaceuticals. Transformations in food habits, less physical activity and increasing desk-oriented jobs have made vulnerable the lifestyle ailments. The common urban and semi-urban populations are becoming more aware about their health and fitness. This is providing a massive growth opportunity for expanding nutraceuticals in India. According to the Associated Chambers of Commerce and Industry of India, the Indian nutraceuticals market is growing from $ 4 Bn in 2015 to $ 10 Bn in 2022. This represents a remarkable growth rate of 21% annually (www.mrssindia.com). Disposal of the spent which amounts to 50–95% of the total quantity of herbs, shrubs, seeds and/or roots processed and together totally termed as Nutraceutical Industrial Spent (NIS) is posing a challenge for the industry. The peculiarity of the spent is that they cannot be used either as manure or as an animal feed due to the chemicals used while processing. Subjecting the spent to use as a fuel in furnace is a feasible proposition, but the problem of environment pollution as greenhouse gases comes as a problem.

Our research school is the first to undertake investigations on the use of NIS as filler material in the fabrication of thermoplastic and thermoset composites (Taqui et al. 2019; Syed and Syed 2016a, b; Syed and Syed 2012; Pashaei et al. 2011; Syed et al. 2010a, b, 2011; Syed et al. 2009). We have also taken a lead in using NIS as adsorbent for remediation of Congo red, methylene blue and ethidium bromide dyes (Taqui et al. 2017; Papegowda and Syed 2017; Sulthana et al. 2018). Despite myriad research papers reporting on the use of low-cost agricultural waste materials as biosorbents for the remediation of toxic dyes, very limited information is available on the utilization of dye-adsorbed biosorbent or 'sludge.' We have directed our effort also on the use of 'sludge' as filler material in the fabrication of thermoplastics and thermosets (Taqui et al. 2019).

Seeds of fenugreek (*Trigonella foenum-graecum L.*, Leguminosae family) have been categorized as nutraceuticals. It is the oldest medicinal plant, originated in India and as well as in North Africa. It is an annual plant, growing about two feet height. Both leaves and seeds are used for extraction. The powder of fenugreek seeds is also used as medicine. The plant extract possesses many therapeutic properties, of which pain relief, anti-inflammation, laxative and antispasmodic are important. It is also used as

Fig. 1 **a** Fenugreek seed and **b** nutraceutical industrial fenugreek seed spent

(a) Fenugreek Seed

(b) Nutraceutical Industrial Fenugreek Seed Spent

anticancer and diabetic carminative, heart tonic, hypertension decreasing, triglyceride lowering, breast milk increasing, oxytocic and sexual desire enhancer (Smith 2003).

India is the largest producer of fenugreek in the world, and the average production during 2011–12 was 121,775 tons (Vidyashankar 2014). The seed is traded as a spice and oil extracted as oleoresin. Oleoresin constitutes about 50% of the total weight of fenugreek seed. The remaining portion of the seed is discarded as spent, commonly known as nutraceutical industrial fenugreek seed spent (NIFGS). The porous structure of spent traps moisture and decreases the calorific value. This property has, however, been exploited to use it as a potential adsorbent for remediation of AB113 dye from water. Images of fenugreek seeds and fenugreek seed spent are shown in Fig. 1a, b, respectively.

Materials and methods

Materials

Acid blue 113 (AB113) was procured from Sigma-Aldrich, India. Chemical formula $= C_{32}H_{21}N_5Na_2O_6S_2$; molecular weight $= 681.65$; absorbance maximum $(\lambda_{max}) = 566$ nm. The structure of AB113 dye is shown in Fig. 2.
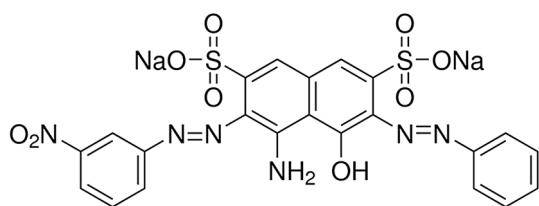

Fig. 2   Structure of Acid blue 113

Table 1   Factors considered for experimental design along with their high and low levels

Factor	Name	Units	Minimum	Maximum
A	Time	min	0	180
B	Temperature	°C	27	50
C	Concentration	mg L^{-1}	25	500
D	Particle size	μ	90	710
E	Adsorbent dosage	g L^{-1}	0.500	6.000
F	pH		2	12

Adsorbent preparation and characterization

Adsorbent preparation

NIFGS procured from a local factory was initially dried in sunlight, crushed and finally ground using a ball mill and sieved to get ASTM standard particle size: (≤ 90, $\geq 90 \leq 125$, $\geq 125 \leq 177$, $\geq 177 \leq 355$, $\geq 355 \leq 500$, $\geq 500 \leq 710$ μm).

Surface characterization, batch adsorption experiments, adsorption kinetics and statistical optimization of process parameters

The experimental details regarding surface characterization (SEM, IR and point of zero charge), batch adsorption experiments, adsorption isotherms, adsorption kinetics and statistical optimization of process parameters are shown in Table 1, and the details are reported elsewhere (Dhaif-Allah et al. 2019).

Results and discussion

Characterization of the adsorbent

Surface characterization of NIFGS done through SEM exhibited slightly porous structure (Fig. 3a). Upon

Fig. 3 a SEM image of NIFGS and **b** SEM image of AB113 adsorbed NIFGS

(a) SEM image of NIFGS
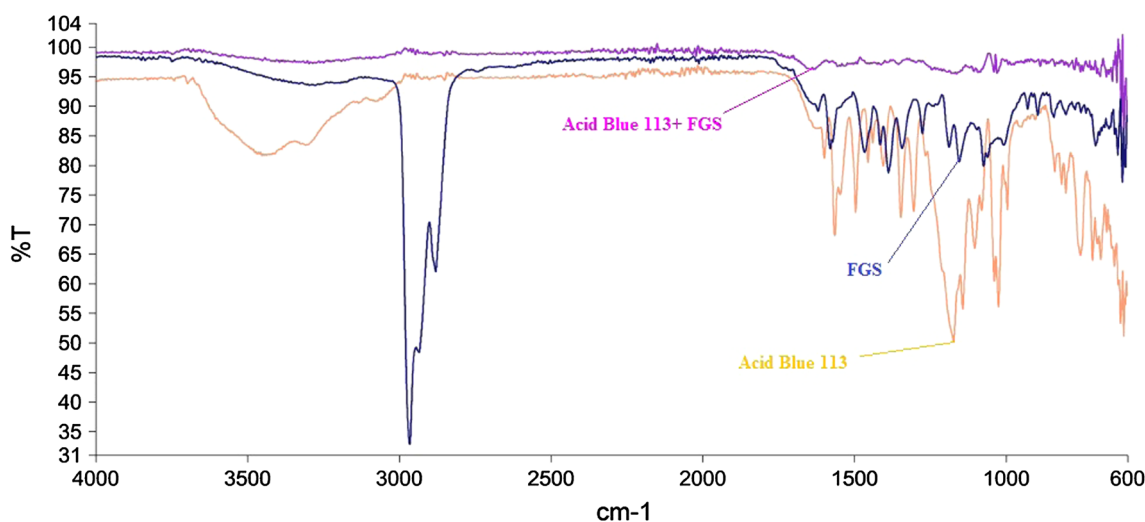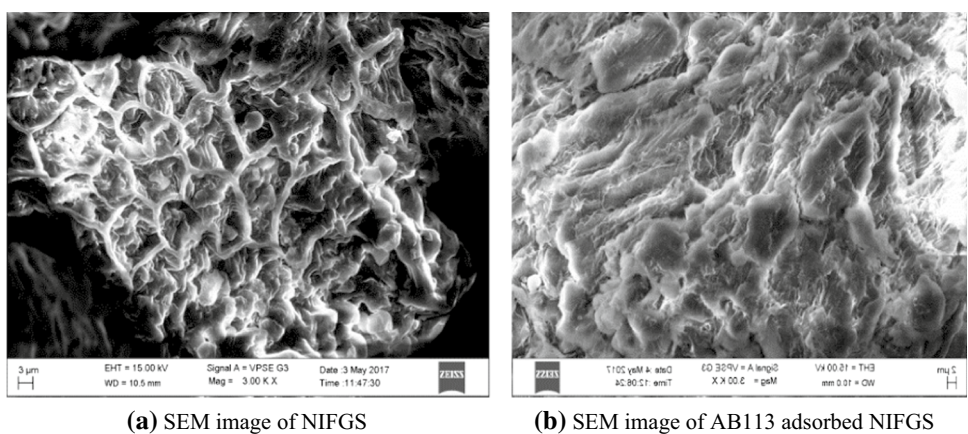

(b) SEM image of AB113 adsorbed NIFGS

Fig. 4 FTIR spectra of AB113, NIFGS and AB113 adsorbed on NIFGS

adsorption (Fig. 3b) of AB113 dye, some pores got completely filled with the adsorbate forming a thin film over the particle. IR spectra of NIFGS (Fig. 4) provided that the absorption at 3299 cm^{-1} is due to stretching of hydroxyl groups of cellulose, hemicellulose and lignin present in NIFGS. The band at 2967 cm^{-1} is due to the C–H stretching of saturated carbon. The bands at 1635 cm^{-1} are due to C=C stretching. The bands at 1163 cm^{-1} and 1038 cm^{-1} are assigned to C–O vibrations and O–H bending, respectively. The finger print region of the biological material NIFGS indicates complex bands, and accurate assignment of the peaks is difficult in the absence of standard sample. However, the presence of cellulose and lignin indicates that the spent has hydrophilic and hydrophobic properties. Determination of point of zero charge at intersection of two plots (Fig. 5) confirms that at pH 7.1 the adsorbent surface has zero charge.
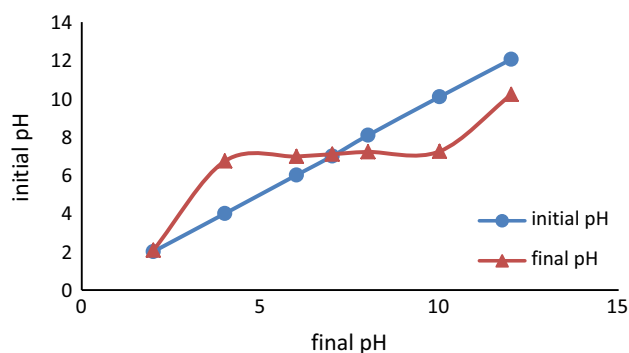

Fig. 5 Point of zero charge of NIFGS at the intersection

Effect of pH, initial dye concentration, adsorbent dosage, adsorbent particle size and temperature

The effect of different parameters on batch adsorption studies of NIFGS had shown remarkable similarities

with our earlier reported studies (Dhaif-Allah et al. 2019). Adsorption capacity observed at pH 2 was maximum (Fig. 6a), and significant decrease in adsorption occurred when pH was increased from 2 to 4. Thereafter, marginal change in adsorption was noticed up to pH 12. Maximum AB113 dye removal by NIFGS was at pH 2.0 ($q_e = 91.00$ mg g^{-1}) with initial concentration of 100 µg ml^{-1}. Initial dye concentration versus q_e and % q_e is shown in Fig. 6b. The effect of adsorbent dosage was similar to the studies reported by us (Dhaif-Allah et al. 2019). The results are illustrated in Fig. 6c. Adsorption capacity was maximum for initial AB113 dye concentration of 100 µg ml^{-1} at neutral pH. The particle size of ≤ 90 µm; ≥ 90 µm ≤ 125 µm; ≥ 125 µm ≤ 177 µm;

≥ 177 µm ≤ 355 µm; ≥ 355 µm ≤ 500 µm and ≥ 500 µm ≤ 710 µm in which the adsorption of dye decreased with the increase in the size of the adsorbent particle size (Fig. 6d). The observation is in conformity with the universal fact that surface area decreases with increase in particle size. The size ≥ 125 µm ≤ 177 µm (80 mesh ASTM) was selected for further studies because 80 mesh particle is commonly used in the fabrication of composites and sieving lower size particles takes more time and adds additional cost to the process. The influence of temperature on adsorption was studied at 30–50 °C with three dye concentrations. Figure 6e shows that increase in temperature decreases adsorption rate indicating that it is an endothermic process (Chowdhury and Das 2012).
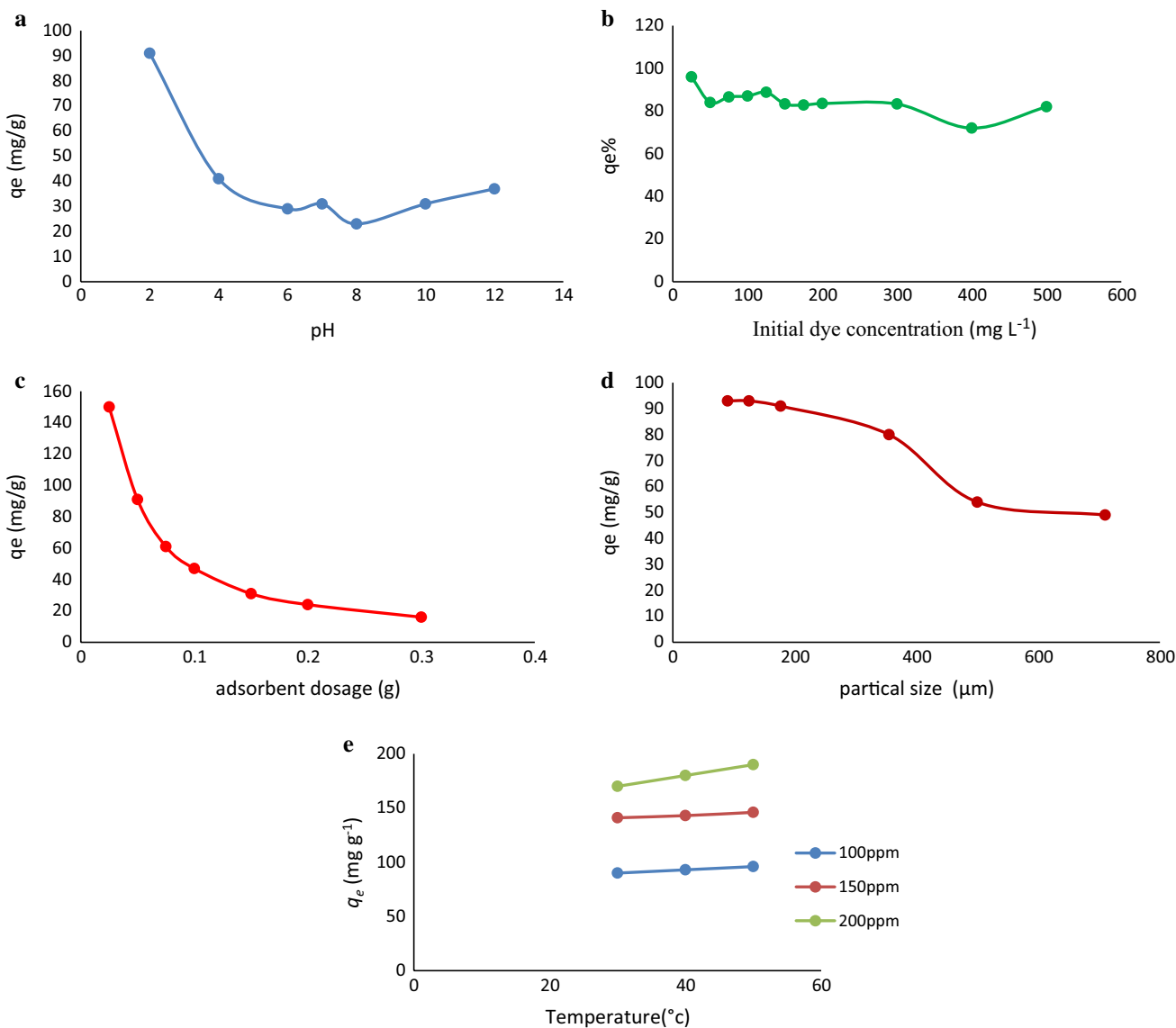

Fig. 6 Effect of **a** pH, **b** initial dye concentration, **c** adsorbent dosage, **d** particle size and **e** temperature onto adsorption of dye onto AB113-NIFSS system
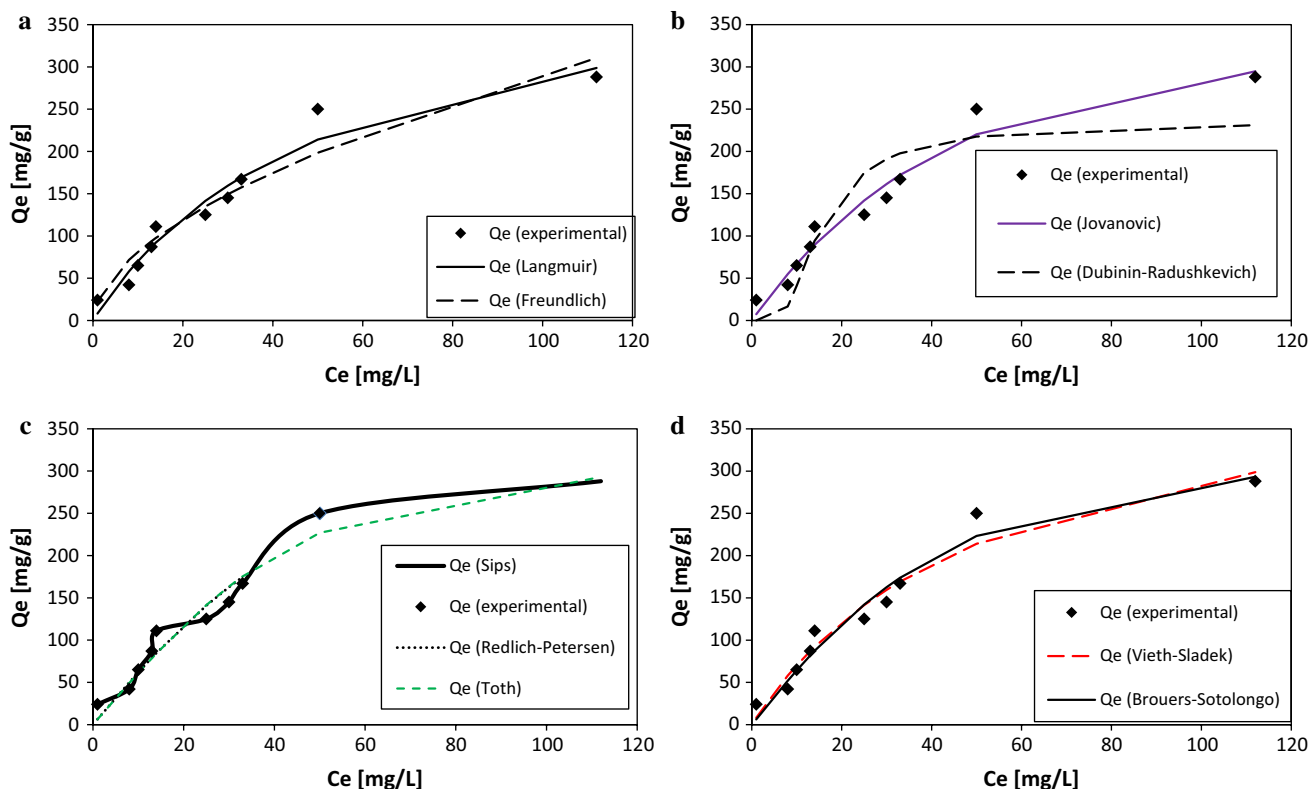
Fig. 7 Fitting of adsorption data to **a** Langmuir and Freundlich, **b** Jovanovic and Dubinin–Radushkevich, **c** Sips, Redlich–Petersen and Toth and **d** Vieth–Sladek and Brouers–Sotolongo adsorption isotherms

Table 2 Calculated parameters of two-parameter isotherms

Two-parameter isotherms							
Langmuir		Freundlich		Jovanovic		Dubinin–Radushkevich	
Q_m	439.06	K_F	22.52	Q_m	316.94	Q_s	234.59
K_S	0.019	n_F	1.798	K_J	0.024	K_{ad}	3.01E−05

Table 3 Calculated parameters of three-parameter isotherms

Three-parameter isotherms									
Redlich–Peterson		Toth		Sips		Vieth–Sladek		Brouers–Sotolongo	
A_{RP}	6.38	Q_m	317.45	Q_m	413.09	Q_m	439.06	Q_m	308.16
B_{RP}	0.001	n_{T0}	2.142	K_s	0.028	K_{VS}	1.0E−07	K_{BS}	0.020
g	1.596	b_{T0}	4603.28	m_s	1.212	β_{VS}	0.019	α	1.062

Table 4 Statistical parameters for isotherm model fitting

Isotherms	Langmuir	Freundlich	Jovanovic	Dubinin–Radushkevich	Redlich–Peterson	Toth	Sips	Vieth–Sladek	Brouers–Sotolongo
SSE	2779.9	4774.2	2421.4	11912.0	2250.5	2403.1	2707.6	2779.9	2381.6
χ^2	29.286	40.914	27.640	91.021	27.968	29.013	30.890	29.286	28.533
R^2	0.96	0.93	0.96	0.856	0.97	0.97	0.96	0.96	0.97

Adsorption isotherm

Adsorption isotherm parameters are useful to know the interactions of adsorbate molecules with adsorbent surface. This is achieved through Langmuir and Freundlich isotherm models by predicting the adsorption capacities. The implication of Langmuir isotherm model is that the adsorption process is monolayer process which happens on the surface of adsorbent, and it involves finite number of similar adsorption sites processing uniform energies (Langmuir 1916). The equation used for this is as follows:

$$q_e = \frac{Q_m K_a C_e}{1 + K_a C_e} \quad R_L = \frac{1}{1 + K_a C_0} \tag{1}$$

Here, q_e implies quantity of dye adsorbed by adsorbent (mg g^{-1}) under equilibrium condition; C_e is the equilibrium concentration (µg ml^{-1}). Intercept and slope of q_e versus C_e determine the value of Q_m and K_a, The monolayer adsorption capacity (mg g^{-1}) is determined by Q_m, and K_a is the Langmuir constant (L mg^{-1}) which has relation to free energy of adsorption. The equilibrium experiments conducted with initial AB113 concentrations of 25–400 µg ml^{-1} gave the Q_m value as 439.06 mg g^{-1} for the isotherm, and it is higher compared to experimental q_e value of 91.00 mg g^{-1}. But, the R^2 value of 0.96 infers a good fitting of this isotherm to the experimental data. The R_L separation factor of the Langmuir isotherm (Webber and Chakkravorti 1974) was between 0.677 and 0.116, indicating favorable adsorption of AB113 on to NIFGS. The values of R_L indicate whether the adsorption is unfavorable ($R_L > 1$), linear ($R_L = 1$), favorable ($0 < R_L < 1$) or irreversible ($R_L = 0$). Lowering of R_L with consequent increase in initial concentration indicates higher adsorption at higher temperature. The large difference between Q_m (439.06 mg g^{-1}) and q_e (91.00 mg g^{-1}) is not very much favorable. Hence, Freundlich isotherm model was tried.

Freundlich isotherm model suggests that the adsorption process takes place on a heterogeneous surface (Freundlich 1906). In the present study, the adsorption capacity of NIFGS is related to AB113 dye concentration at equilibrium, and this is shown by following equation:

$$q_e = K_F C_e^{1/n_F} \tag{2}$$

Here, K_F and n_F signify Freundlich constants in relation to capacity for adsorption [mg g^{-1}] and intensity of adsorption [mg/L]$^{-1/n}$, respectively. Heterogeneity factor (n_F) is the name for latter. This indicates whether the adsorption is linear ($n_F = 1$), chemisorption ($n_F < 1$) or physisorption ($n_F > 1$). The values of n_F and $1/n_F$ in the present study are 1.798 and 0.556, respectively, which indicate that the process is physisorption. K_F and n_F are calculated from the intercept and slope of the plot ln q_e versus ln C_e. The fitting of Freundlich isotherm to the experimental data has given a R^2 value of 0.93 which implies that it is linear process. Hence, the adsorption of AB113 dye on to NIFGS is favorable and the process is physisorption. But from Langmuir and Freundlich models, no definite inference was obtained with respect to homogeneity or heterogeneity of the process of adsorption. Therefore, Jovanovic isotherm (Jovanović 1969) model was tried and the equation for Jovanovic model is

$$q_e = Q_m(1 - e^{(K_J C_e)}) \tag{3}$$

K_j represents Jovanovic constant, q_e is the quantum of dye adsorbed on to adsorbent (mg g^{-1}) at equilibrium; equilibrium concentration (µg ml^{-1}) of dye in solution is represented by C_e. This model signifies monolayer formation having no interactions. Deviation of results from Langmuir isotherm is denoted by Kj. According to this model, the value of Q_m obtained is 316.94 mg g^{-1}, which is higher than 91.00 mg g^{-1} obtained by the experiment. But it is lower than that obtained by Langmuir isotherm.

Table 5 Experimentally determined and theoretically predicted parameters for absorption kinetic models

Initial concentration (ppm)	Temp (K)	Qe_{expt} (mg g^{-1})	Pseudo-first order				Pseudo-second order			
			Qe_{pred} (mg g^{-1})	k_1	R^2	χ^2	Qe_{pred} (mg g^{-1})	k_2	R^2	χ^2
100	303	90	79.43	3.16E−01	0.44	3.08	84.23	6.86E−03	0.78	2.21
	313	93	79.43	2.64E−01	0.43	5.06	82.43	6.58E−03	0.73	2.59
	323	96	83.37	2.04E−01	0.72	4.07	91.95	3.42E−03	0.93	1.06
150	303	141	176.38	6.90E−02	0.89	19.89	213.78	3.73E−04	0.91	12.97
	313	143	176.47	1.76E+02	0.88	20.22	65.88	1.71E−03	0.76	1.65
	323	146	181.42	7.33E−02	0.90	17.83	218.26	3.97E−04	0.92	10.93
200	303	170	260.13	1.25E−01	0.92	6.77	297.90	5.52E−04	0.96	4.84
	313	180	271.60	1.12E−01	0.96	4.90	314.03	4.60E−04	0.98	3.35
	323	190	277.84	1.37E−01	0.98	2.04	313.11	6.15E−04	0.97	3.07

Table 6 Calculated parameters for diffusion models

Initial concentration (ppm)	Temp (K)	Film diffusion model		Weber–Morris model		Dumwald–Wagner	
		$R|$ (min^{-1})	R^2	k_{ist} (mg g^{-1} s$^{-0.5}$)	R^2	K (min^{-1})	R^2
100	303	0.0303	0.97	3.48	0.98	0.030	0.90
	313	0.0321	0.92	4.40	0.97	0.028	0.96
	323	0.0384	0.99	5.60	0.97	0.035	0.99
150	303	0.0059	0.98	3.20	0.98	0.005	0.98
	313	0.0144	0.98	7.19	0.97	0.012	0.97
	323	0.0341	0.99	9.99	0.98	0.020	0.98
200	303	0.0057	0.87	4.21	0.93	0.004	0.88
	313	0.0081	0.87	5.53	0.91	0.007	0.88
	323	0.0147	0.97	8.32	0.96	0.016	0.97

The equation for the isotherm model proposed by Dubinin–Radushkevich (Dubinin 1947) is as follows:

$$q_e = q_s[\exp(-K_{ad}\varepsilon^2)] \quad \text{where} \quad \varepsilon = RT \ln\left[1 + \frac{1}{C_e}\right]. \quad (4)$$

In this equation, q_s (mg g^{-1}) has relation to adsorption capacity q_e (mg g^{-1}), K_{ad} (mol^2 kJ^{-2}) is the average free energy of adsorption, R (J mol^{-1} K^{-1}) and T (K) is denoted by absolute temperatures. The value realized is Q_m=234.59 mg g^{-1} which is higher than the experimental value of q_e = 91.00 mg g^{-1}. R^2 value, which indicates linearity, is 0.86. However, as the values of χ^2 and R^2 are closer, it is a better fit model than Langmuir model (Fig. 7a, b). The results presented in Tables 2, 3 and 4 prove that AB113 dye interacts with NIFGS linearly, and the reaction is physical and favorable.

Toth, Sips, Radke–Prausnitz, Redlich–Peterson, Vieth–Sladek and Brouers–Sotolongo are six other three-parameter isotherm models which were also tried for academic interest.

The Toth isotherm (Toth 1971) is useful for heterogeneous adsorption system. In Table 4 and Fig. 7c, Q_m value of 317.45 mg g^{-1} obtained is higher compared to experimental q_e value of 91.00 mg g^{-1} but lower to Langmuir isotherm value of 439.06 mg g^{-1}.

Sips isotherm (Sips 1948) depending upon the adsorbate concentration can be either Langmuir or Freundlich isotherm equation. The value Q_m=413.09 mg g^{-1} in Sips isotherm deviates from experimental value R^2=0.96, SSE of 2707.6 and χ^2 of 30.89 values making it a good fit.

The Redlich–Peterson isotherm model (Redlich and Peterson 1959) is improved version of Langmuir–Freundlich, and a correction factor 'g' is included. In the equation, Langmuir isotherm represents $g=1$ and Freundlich isotherm is $g=0$ and the 'g' value of 1.596 obtained indicates that adsorption is tending toward Langmuir isotherm. The equation of Redlich–Peterson isotherm is given as:

$$q_e = \frac{A_{RP}C_e}{1 + B_{RP}C_e^g} \quad (5)$$

A_{RP}, B_{RP} and g are Redlich–Peterson constants, q_e is the quantity of dye being adsorbed (mg g^{-1}) under equilibrium; equilibrium concentration (µg ml^{-1}) of dye in solution is represented by C_e.

Vieth–Sladek isotherm (Vieth and Sladek 1965) is useful for such solutes which get adsorbed as per some specific isotherms which simplify linear component (Henry's law) and nonlinear components (Langmuir equation) according to solute dissolved in adsorbents amorphous region. This model estimates rates of diffusion from transient adsorption in solid materials. The equation of this isotherm is:

$$q_e = K_{VS}C_e + \frac{Q_m \beta_{VS} C_e}{1 + \beta_{VS} C_e} \quad (6)$$

K_{VS} and β_{VS} are Vieth–Sladek constants, q_e is the quantity of dye being adsorbed by the adsorbent (mg g^{-1}) under equilibrium condition, maximum adsorption capacity is Q_m, and C_e is the equilibrium concentration (µg ml^{-1}) of the dye. In this study, the SSE value got is 2779.9, χ^2 is 29.286 and R^2 is 0.96. These make a good fit to the experimental values. The Q_m value obtained is 439.06 mg g^{-1}.

Brouers–Sotolongo isotherm (Brouers et al. 2005) is similar to that of Vieth–Sladek isotherm. The K_{BS} and α in the equation represent adsorption power and active site distribution, respectively, of the adsorbent–adsorbate system. The equation is:

$$q_e = Q_m[(1 - \exp(-K_{BS}(C_e)^\alpha)] \quad (7)$$

Here, K_{BS} and α are Brouers–Sotolongo constants, amount of dye adsorbed by adsorbent (mg g^{-1}) at equilibrium is denoted by q_e, Q_m is the maximum adsorption capacity, and equilibrium concentration (µg ml^{-1}) of the dye in

Fig. 8 Kinetic model fits for, **a** 100 μg ml^{-1}, **b** 150 μg ml^{-1} and **c** 200 μg ml^{-1} initial dye concentration of AB113 on NIFGS system at different temperatures
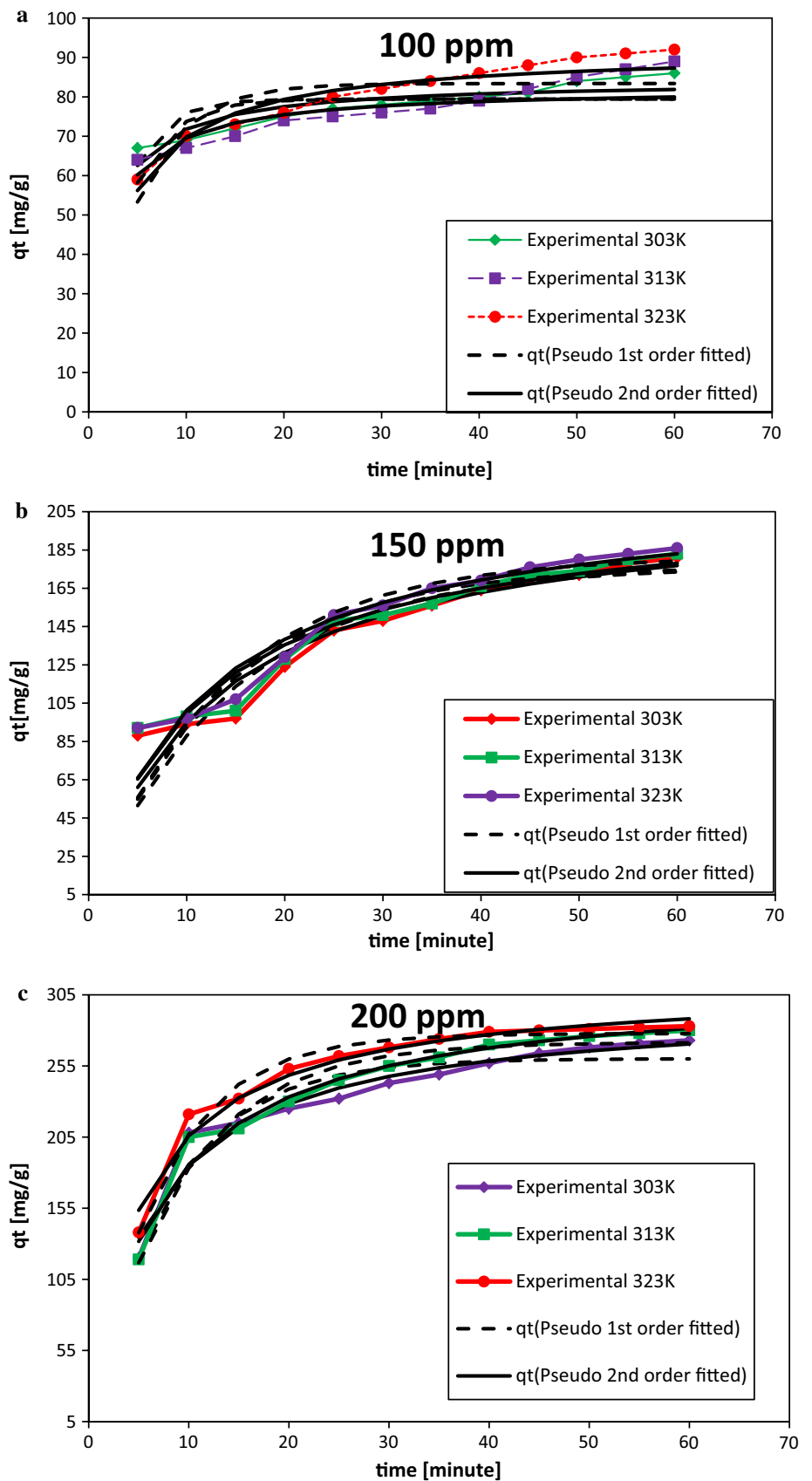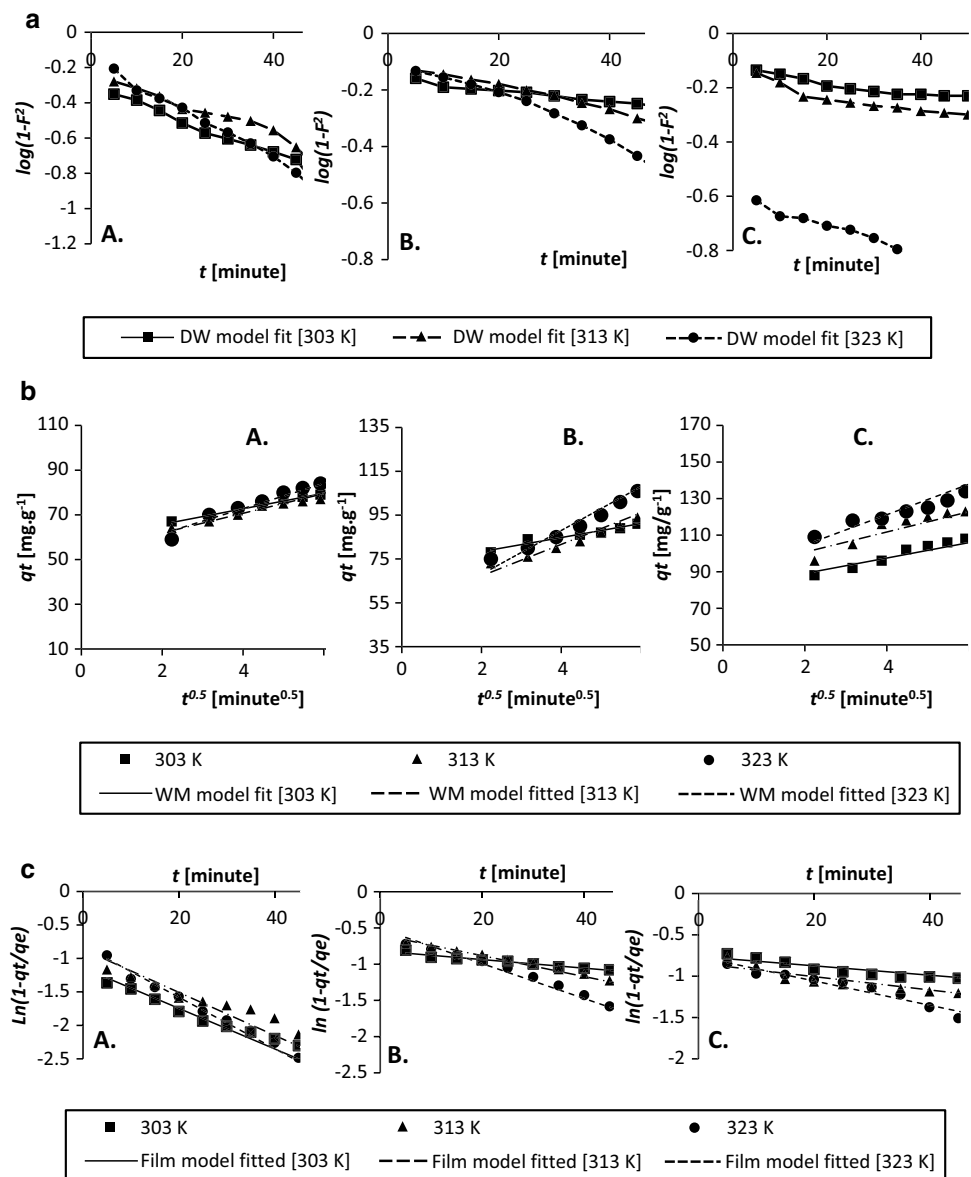
Fig. 9 Kinetics data fitted to **a** Dumwald–Wagner, **b** Weber–Morris and **c** film diffusion models with initial concentration of AB113 dye: (A) 100 µg ml^{-1}, (B) 150 µg ml^{-1}, (C) 200 µg ml^{-1}

Adsorption kinetics

solution is indicated by C_e. The value of Q_m obtained is 108.00 mg g^{-1} which is slightly higher than the experimental result of 91.00 mg g^{-1}, and the R^2 value of 0.97 is a good prediction to the experimental data (Fig. 7d).

These models discuss about more complicated equations but they definitely help in making the mechanism of adsorption more clear. The value of R^2 alone cannot be considered for the experiment since it can be applied only for linear models. χ^2 values, however, are applicable only if model data and experimental data are similar. The Q_m, χ^2 and R^2 values of all the nine models are presented in Tables 4 and 5. The values of all these models as also the actual experimental data (q_e) will provide useful guidance for further research to develop new models in solving adsorption phenomena occurring in AB113-NIFGS system.

Kinetic data obtained at 100, 150 and 200 µg ml^{-1} concentrations of AB113 dye and at 303 K, 313 K and 323 K temperature were analyzed using models proposed by Lagergren (1898), Ho and McKay (1998), Alkan et al. (2007), Wang et al. (2004) and Boyd et al. (1947) to collect information about their effect on adsorption rate. The parameters tested were analyzed by nonlinear analyses (MS Excel 2010), and the results are presented in Table 6. Pseudo-second-order model proposed by Ho and McKay has given the best fit at all the tested dye concentrations and temperatures investigated as evidenced by coefficient of determination (R^2) and chi-square (χ^2) values (Fig. 8a–c). Maximum adsorption took place in the beginning which gradually slowed down

Fig. 10 a Plot of thermodynamic equilibrium constant versus $1/T$ to determine the enthalpy and Gibbs free energy of the process. **b** Plot of pseudo-second-order kinetic constant versus $1/T$ to determine the activation energy of the process
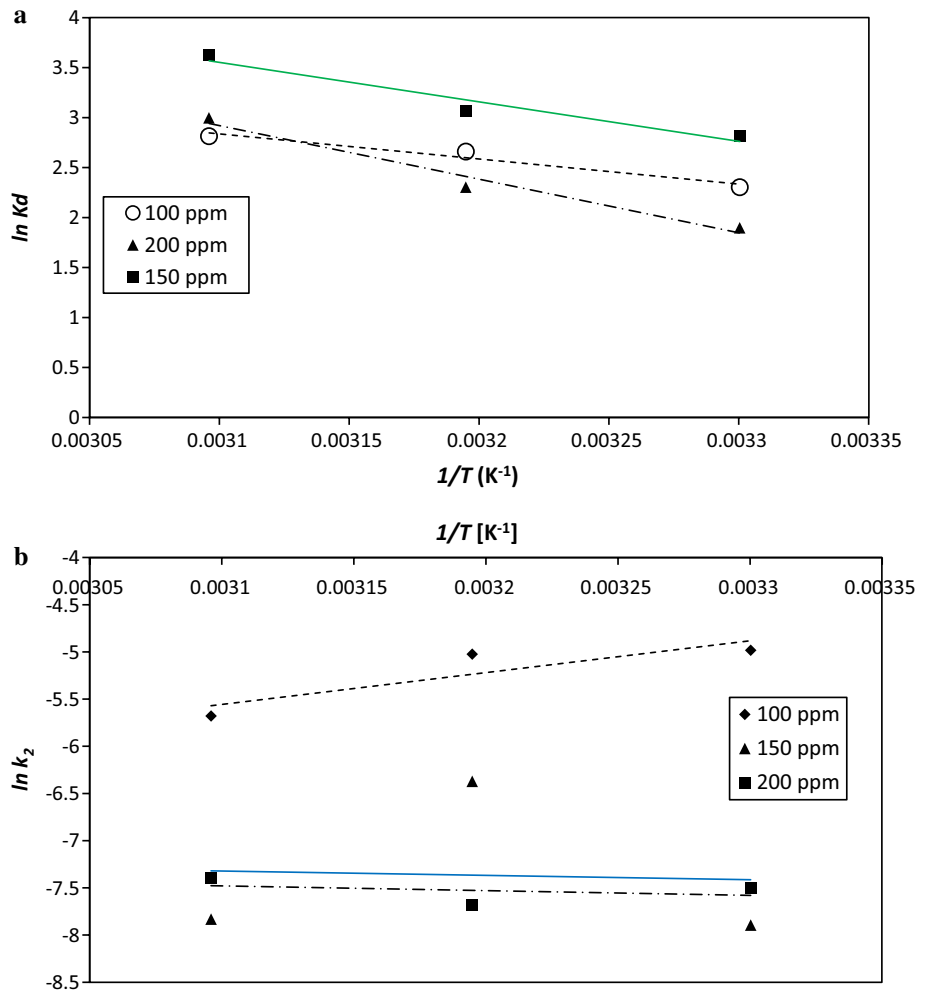

Table 7 Thermodynamic parameters of AB 113-FGS system

Initial concentration	Temperature	$\Delta G°$	$\Delta S°$	$\Delta H°$	$\ln A$	E_a
(ppm)	(K)	(kJ mol^{-1})	(J mol^{-1} K^{-1})	(kJ mol^{-1})		(kJ mol^{-1})
100	303	-5.80	733.67	173.46	-16.01	-233.16
	313	-6.92				
	323	-7.56				
150	303	-7.09	1092.07	273.09	-5.89	31.83
	313	-7.98				
	323	-9.73				
200	303	-4.78	1350.10	370.44	-5.92	
	313	-5.99				34.84
	323	-8.04				

Table 8 ANOVA for fractional factorial experimental design

Source	Sum of squares	Degree of freedom	Mean square	F value	P value
Model	310699.1	15	20713.3	326.1	<0.001**
A	31434.3	1	31434.3	494.9	<0.001**
B	4393.0	1	4393.0	69.2	<0.001**
C	47483.2	1	47483.2	747.6	<0.001**
D	2620.5	1	2620.5	41.3	<0.001**
E	8932.6	1	8932.6	140.6	<0.001**
F	2720.8	1	2720.8	42.8	<0.001**
AB	191.5	1	191.5	3.0	0.0847+
AC	10187.6	1	10187.6	160.4	<0.001**
BC	2081.9	1	2081.9	32.8	<0.001**
A^2	6268.0	1	6268.0	98.7	<0.001**
B^2	64.6	1	64.6	1.0	0.3149
C^2	70.7	1	70.7	1.1	0.2930
D^2	0.6	1	0.6	0.0	0.9224
E^2	2767.5	1	2767.5	43.6	<0.001**
F^2	2941.0	1	2941.0	46.3	<0.001**
Residual	8955.2	141	63.5		

Suggestive significance (p value: $0.05 < p < 0.10$)

Moderately significant (p value: $0.01 < p \leq 0.05$)

** Strongly significant (p value: $p \leq 0.01$)

and thereafter remained almost constant. Higher temperature increased adsorption capacity (q_e) marginally. The AB113 dye molecules moved from solution to the solid surface and then diffused into the pores of NIFGS. Thus, it may be inferred that multi-step adsorption which is not rate limiting has occurred. The observations made using Dumwald–Wagner model (Fig. 9a), Weber–Morris model (Fig. 9b) and film diffusion model (Fig. 9c) were similar to our earlier studies (Dhaif-Allah et al. 2019). The data in Table 6 conclusively prove that diffusion is a rate-limiting process.

Adsorption thermodynamics

The thermodynamic parameters including $\Delta H°$, $\Delta S°$ and E_a which were estimated using the slope and intercept of Van't Hoff plots of $\ln(K_d)$ and $\ln(K_2)$ versus $1/T$ are shown in Fig. 10a, b, respectively, and presented in Table 7. The interpretation of the data is as described in our paper (Dhaif-Allah et al. 2019). The activation energy values for initial concentrations of 100, 150 and 200 μg ml^{-1} as obtained by applying kinetic constant from pseudo-second-order model and Arrhenius equation ranged between ~ − 233.16 and 34.84 kJ mol^{-1}.

Fig. 11 2D-contour plot and 3D-surface plot showing the variation of ▶ adsorption capacity with **a** time versus concentration, **b** temperature versus pH, **c** time versus adsorbent dosage and **d** concentration versus particle size

Statistical optimization by fractional factorial experimental design (FFED)

The statistical optimization of six parameters (independent variables), including the time of interaction of AB113 dye solution (adsorbate) with NIFGS dosage and particle size (adsorbent), temperature and time of interaction process between adsorbent and adsorbate, initial dye concentration and pH of the solution and their effects on adsorption process of dependent variable, namely q_e (adsorption equilibrium) using FFED resulted in arriving at a quadratic equation as shown below (Eq. 8)

$$\text{Adsorption} = 38.2 + 65.3 * A + 23.5 * B + 143.3$$
$$* C - 25.4 * D - 45.9 * E - 24.0 * F + 2.7$$
$$* AB + 67.9 * AC + 30.7 * BC23.0 * A^2 + 1.9$$
$$* B^2 + 6.6 * C^2 + 0.8 * D^2 + 49.2 * E^2 - 40.6 * F^2.$$
(8)

The above quadratic model is useful in predicting the maximum adsorption capacity as also gives idea about the interaction between independent variables and their effect on adsorption process through analysis of variance (ANOVA). The calculations of ANOVA are characterized by computing a number of means and variances, dividing two variances and comparing the ratio to a value to determine statistical significance. The values presented in Table 8 obtained from the quadratic regression analysis clearly show the significance of individual and combined effects of independent variable(s). The values obtained through statistical optimization are 661.50 mg g^{-1} (maximum adsorption), 0.6 g L^{-1} and 321 μm (adsorbent dosage and particle size), 199 min and 52 °C (time and temperature) with orbital shaking of 165 rpm. The effects of two independent variables together on adsorption (the dependent variable) are graphically presented in the contour and surface plots (Fig. 11a–d).

Application of proposed method to textile industrial effluent

A simple procedure was developed to compare the remediation process for AB113 dye in water as also in textile industrial effluent, and these are explained elsewhere (Dhaif-Allah et al. 2019). This procedure was also adopted using NIFGS as adsorbent. Recovery of the dye and allied
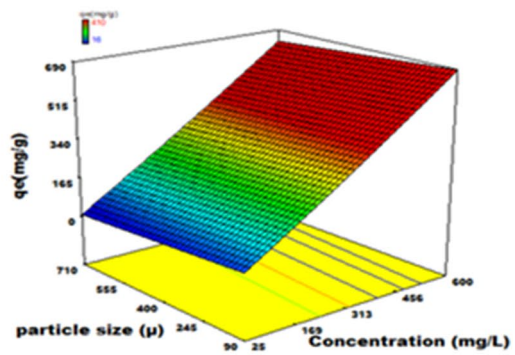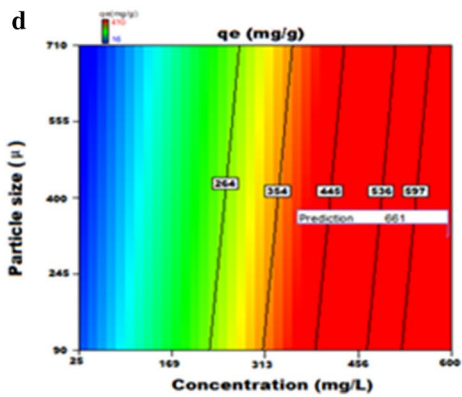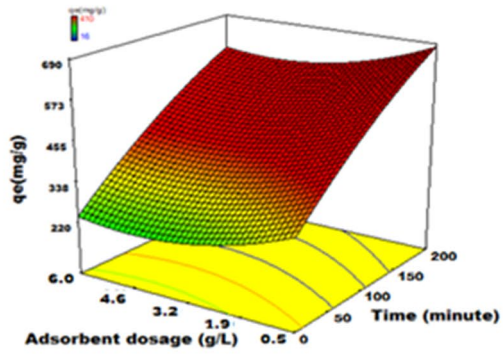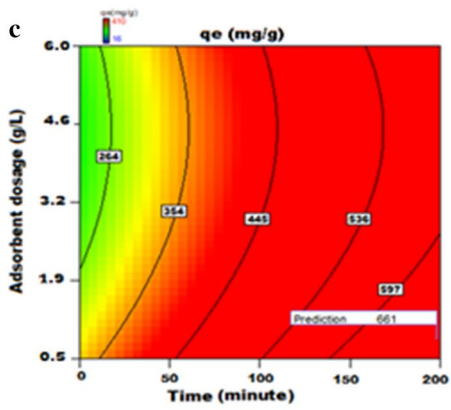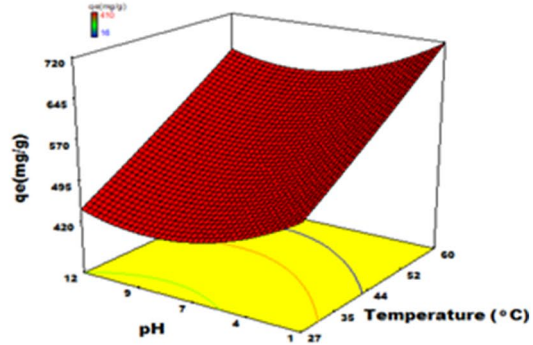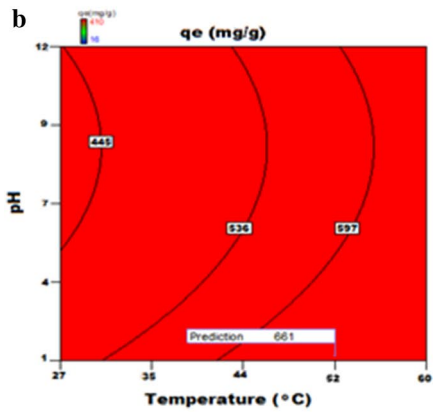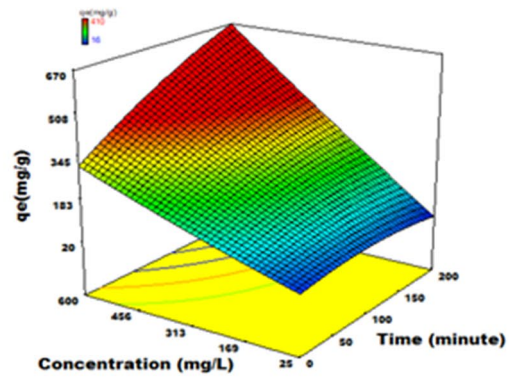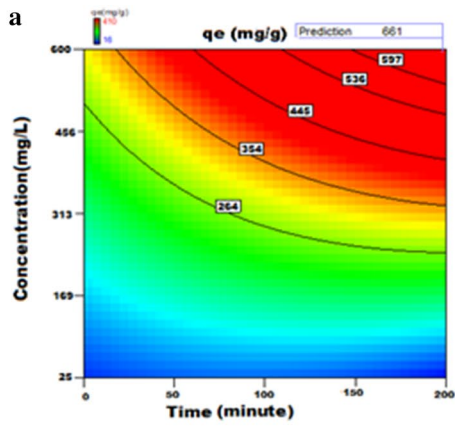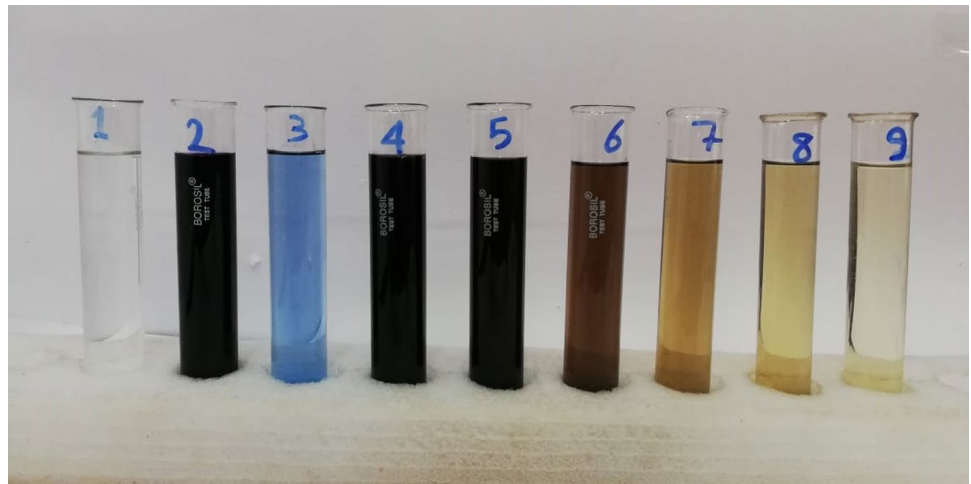
Fig. 12 Color of the solutions before and after adsorption: (1) distilled water, (2) AB113 in distilled water, (3) TIE, (4) AB113 in TIE, (5) filtrate after adsorption of dye on NIFGS after 15 min, (6) 30 min, (7) 45 min, (8) 60 min and (9) filtrate of NIFGS in distilled water

substances to the extent of 75%, 90%, 93% and 95% after 15, 30, 45 and 60 min, respectively, was obtained. This observation is in line with the kinetic results, where the solute gets adsorbed onto the surface quickly forming a film. Later on, the adsorption gets retarded due to the formation of film thereby causing change in absorption rates (Fig. 12). Scaling up of the experiment was done by using 10 g, 20 g and 50 g of NIFGS and using 1, 2 and 5 L of AB113 dye dissolved in TIE. Results did not exceed in all cases $\pm 2\%$ error. The scale up experimental data yielded promising and reliable results about the process which could be extended to a higher scale to operate under industrial environment.

Regeneration of the adsorbent and cost analysis

Dye-adsorbed NIFGS can be regenerated for its reuse along with the recovery of the adsorbed NIFGS. But the proposition may not prove economical because the process and solvents cost will be much higher when compared to the recovered adsorbent cost (< 1 US$ for 50 Kg of NIFGS). In addition, the enhancement of E-factor (Sheldon 1992) is not desirable since it will add to the unprecedented load of environmental toxicants. But in our laboratory, work is in progress to use dye adsorbed nutraceutical industrial spent as filler/reinforcing material and encouraging results have come out and a part of it have been published elsewhere (Taqui et al. 2017, 2019).

Conclusion

The results of research have conclusively proven that use of NIS for the adsorption and remediation of toxic dyes from textile industrial effluent is not only a successful process but also has significant economic payoffs. Use of NIFGS as an adsorbent is an eco-friendly and potentially a low-cost

process for removing toxic dye from aqueous media. Optimization of six physicochemical parameters, namely pH of the solution, initial dye concentration, adsorbent dose, contact time of the adsorbent and the adsorbate and temperature and nine isotherm models studied deduces an experimental value of maximum adsorption $q_e = 91.00$ mg g^{-1}, which is nearest obtained by the Brouers–Sotolongo isotherm model ($Q_m = 108.00$ mg g^{-1}) with the correlation coefficient (R^2) of 0.97. FFED and ANOVA along with statistically developed model for adsorption of AB113 dye onto NIFGS predicted a maximum adsorption of 661.5 mg g^{-1}. The p value < 0.001 surmises that pH and time of contact between the adsorbent and the adsorbate and temperature play important role in enhancing the efficiency of adsorption of the toxic dye on NIFGS. The AB113 dye adsorption on to NIFGS is not only endothermic but also almost spontaneous. It fits well with pseudo-second-order kinetic model; film formed significantly affects intra-particular diffusion. The physical nature of the process is evident by low ΔH value. The adsorption of AB113 dye onto NIFGS was further confirmed by SEM images and FTIR spectra.

Commercialization and utilization of dye-adsorbed spent as filler/reinforcement material(s) in the fabrication of low-cost thermoplastics and thermosets will create more jobs and ecologically alleviate NIS disposal problems in landfills. This clean, cheap and efficient technology for the disposal of spent material from nutraceutical industries will definitely cater to the requirement of sustainability; economic gains, environmental concern and social obligation.

Compliance with ethical standards

Conflict of interest All authors declare no conflict of interest.

References

Alkan M, Demirbaş Ö, Doğan M (2007) Adsorption kinetics and thermodynamics of an anionic dye onto sepiolite. Microporous Mesoporous Mater 101(3):388–396

Boyd GE, Adamson AW, Myers LS Jr (1947) The exchange adsorption of ions from aqueous solutions by organic zeolites. II. Kinetics. J Am Chem Soc 69(11):2836–2848

Brouers F, Sotolongo O, Marquez F, Pirard JP (2005) Microporous and heterogeneous surface adsorption isotherms arising from levy distributions. Physica A Stat Mech Appl 349(1):271–282

Carliell CM, Barclay SJ, Shaw C, Wheatley AD, Buckley CA (1998) The effect of salts used in textile dyeing on microbial decolourisation of a reactive azo dye. Environ Technol 19:1133–1137

Chowdhury S, Das P (2012) Utilization of a domestic waste—eggshells for removal of hazardous malachite green from aqueous solutions. Environ Prog Sustain 31(3):415–425

Dávila-Jiménez MM, Elizalde-González MP, Peláez-Cid AA (2005) Adsorption interaction between natural adsorbents and textile dyes in aqueous solution. Colloids Surf A 254(1–3):107–114

de Lima ROA, Bazo AP, Salvadori DMF, Rech CM, de Palma Oliveira D, de Aragão Umbuzeiro G (2007) Mutagenic and carcinogenic potential of a textile azo dye processing plant effluent that impacts a drinking water source. Mutat Res 626(1):53–60

Dhaif-Allah MAH, Taqui SN, Syed UT, Syed AA (2019) Development of sustainable acid blue 113 dye adsorption system using nutraceutical industrial *Tribulus terrestris* spent. SN Appl Sci 1(4):330

Dubinin MM (1947) The equation of the characteristic curve of activated charcoal. Dokl Akad Nauk SSSR 55:327–329

Eskandarian M, Mahdizadeh F, Ghalamchi L, Naghavi S (2014) Bio-Fenton process for Acid Blue 113 textile azo dye decolorization: characteristics and neural network modeling. Desalin Water Treat 52(25–27):4990–4998

Freundlich HMF (1906) Over the adsorption in solution. J Phys Chem 57:385–471

Green FJ (1990) The Sigma-Aldrich handbook of stains, dyes and indicators. Aldrich Chemical Co, St. Louis

Gupta VK, Gupta B, Rastogi A, Agarwal S, Nayak A (2011) A comparative investigation on adsorption performances of mesoporous activated carbon prepared from waste rubber tire and activated carbon for a hazardous azo dye—Acid blue 113. J Hazard Mater 186(1):891–901

Ho YS, McKay G (1998) Sorption of dye from aqueous solution by peat. Chem Eng J 70(2):115–124

https://www.ibef.org/industry/textiles.aspx. Accessed 28 March 2018

http://www.mrssindia.com/uploads/reports/pdf/assocham-knowledge-report-on-nutracuticalsreleased-at-3rd-national-symposium-6.pdf. Accessed 28 March 2018

Hubbe MA, Hasan SH, Ducoste JJ (2011) Cellulosic substrates for removal of pollutants from aqueous systems: A review. 1. Metals. Bio Resour 6(2):2161–2287

Husain Q, Karim Z, Banday ZZ (2010) Decolorization of textile effluent by soluble fenugreek (*Trigonella foenum-graecum* L.) seeds peroxidase. Water Air Soil Pollut 212(1–4):319–328

Khehra MS, Saini HS, Sharma DK, Chadha BS, Chimni SS (2005) Comparative studies on potential of consortium and constituent pure bacterial isolates to decolorize azo dyes. Water Res 39(20):5135–5141

Lagergren S (1898) About the theory of so-called adsorption of soluble substances. Kungliga Svenska Vetenskapsakademiens Handlingar 24:1–39

Langmuir I (1916) The constitution and fundamental properties of solids and liquids. J Am Chem Soc 38(11):2221–2295

Lee LY, Chin DZB, Lee XJ, Chemmangattuvalappil N, Gan S (2015) Evaluation of abelmoschus esculentus (lady's finger) seed as a novel biosorbent for the removal of acid blue 113 dye from aqueous solutions. Process Safe Environ 94:329–338

Papegowda PK, Syed AA (2017) Isotherm, kinetic and thermodynamic studies on the removal of methylene blue dye from aqueous solution using Saw Palmetto spent. Int J Environ Res 11(1):91–98

Pashaei S, Siddaramaiah, Syed AA (2011) Investigation on mechanical, thermal and morphological behaviors of turmeric spent incorporated vinyl ester green composites. Polym Plast Technol Eng 50(12):1187–1198

Pura S, Atun G (2009) Adsorptive removal of acid blue 113 and tartrazine by fly ash from single and binary dye solutions. Sep Sci Technol 44(1):75–101

Rai CL, Raghav M, Surianarayanan M, Sreenivas V (2013) Kinetic modelling on CI acid blue-113 dye degradation by acoustic and hydrodynamic cavitations. Int J Environ Eng 5(2):208–227

Redlich OJDL, Peterson DL (1959) A useful adsorption isotherm. J Phys Chem 63(6):1024

Saravanan M, Sambhamurthy NP, Sivarajan M (2010) Treatment of acid blue 113 dye solution using iron electrocoagulation. Clean-Soil Air Water 38(5–6):565–571

Sathishkumar P, Mangalaraja RV, Rozas O, Mansilla HD, Gracia-Pinilla MA, Anandan S (2014) Low frequency ultrasound (42 kHz) assisted degradation of acid blue 113 in the presence of visible light driven rare earth nanoclusters loaded TiO$_2$ nanophotocatalysts. Ultrason Sonochem 21(5):1675–1681

Sheldon RA (1992) Organic synthesis-past, present and future. Chem Ind 23:903–906

Shirzad-Siboni M, Jafari SJ, Giahi O, Kim I, Lee SM, Yang JK (2014) Removal of acid blue 113 and reactive black 5 dye from aqueous solutions by activated red mud. J Ind Eng Chem 20(4):1432–1437

Shokohi R, Jafari SJ, Siboni M, Gamar N, Saidi S (2011) Removal of acid blue 113 (AB113) dye from aqueous solution by adsorption onto activated red mud: a kinetic and equilibrium study. Sci J Kurdistan Univ Med Sci 16(2):55–65

Shu HY, Chang MC, Fan HJ (2005) Effects of gap size and UV dosage on decolorization of CI Acid Blue 113 wastewater in the UV/H$_2$O$_2$ process. J Hazard Mater 118(1–3):205–211

Shu HY, Chang MC, Chen CC, Chen PE (2010) Using resin supported nano zero-valent iron particles for decoloration of acid blue 113 azo dye solution. J Hazard Mater 184(1–3):499–505

Shu HY, Chang MC, Huang SW (2015) UV irradiation catalyzed persulfate advanced oxidation process for decolorization of acid blue 113 wastewater. Desalin Water Treat 54(4–5):1013–1021

Shu HY, Huang SW, Tsai MK (2016a) Comparative study of acid blue 113 wastewater degradation and mineralization by UV/

persulfate and UV/Oxone processes. Desalin Water Treat 57(60):29517–29530

Shu HY, Chang MC, Huang SW (2016b) Decolorization and mineralization of azo dye acid blue 113 by the UV/Oxone process and optimization of operating parameters. Desalin Water Treat 57(17):7951–7962

Shu HY, Chang MC, Liu JJ (2016c) Reductive decolorization of acid blue 113 azo dye by nanoscale zero-valent iron and iron-based bimetallic particles. Desalin Water Treat 57(17):7963–7975

Sips R (1948) Combined form of langmuir and freundlich equations. J Chem Phy 16(429):490–495

Smith M (2003) Therapeutic applications of fenugreek. Altern Med Rev 8(1):20–27

Srinivasan R, Mishra A (2008) Okra (*Hibiscus esculentus*) and fenugreek (*Trigonella foenum graceum*) mucilage: characterization and application as flocculants for textile effluent treatments. Chin J Polym Sci 26(06):679–687

Standard methods for the examination of water and wastewater (2002) 20th edn. American Public Health Association, Washington

Sulthana R, Taqui SN, Zameer F, Taqui SU, Syed AA (2018) Adsorption of ethidium bromide from aqueous solution on to nutraceutical industrial fennel seed spent: kinetics and thermodynamics modeling Studies. Int J Phytoremediation 20(11):1075–1086

Syed MA, Syed AA (2012) Development of a new inexpensive green thermoplastic composite and evaluation of its physico-mechanical and wear properties. Mater Des 36:421–427

Syed MA, Syed AA (2016a) Development of green thermoplastic composites from Centella spent and study of its physicomechanical, tribological, and morphological Characteristics. J Thermoplast Compos Mater 29(9):1297–1311

Syed MA, Syed AA (2016b) Investigation on physicomechanical and wear properties of new green thermoplastic composites. Polym Compos 37(8):2306–2312

Syed MA, Siddaramaiah Suresha B, Syed AA (2009) Mechanical and abrasive wear behavior of coleus spent filled unsaturated polyester/polymethyl methacrylate semi interpenetrating polymer network composites. J Compos Mater 43(21):2387–2400

Syed MA, Ramaraj B, Akhtar S, Syed AA (2010a) Development of environmentally friendly high density polyethylene and turmeric spent composites: physicomechanical, thermal, and morphological studies. J Appl Polym Sci 118(2):1204–1210

Syed MA, Siddaramaiah Syed RT, Syed AA (2010b) Investigation on physico mechanical properties, water, thermal and chemical ageing of unsaturated polyester/Turmeric spent composites. Polym Plast Technol Eng 49(6):555–559

Syed MA, Akhtar S, Syed AA (2011) Studies on the physico-mechanical, thermal and morphological behaviors of high density polyethylene/coleus spent green composites. J Appl Polym Sci 119(4):1889–1895

Szyguła A, Guibal E, Ruiz M, Sastre AM (2008) The removal of sulphonated azo-dyes by coagulation with chitosan. Colloids Surf A 330(2–3):219–226

Talwar K, Kini S, Balakrishna K, Murty VRC (2016) Statistical analysis of acid blue-113 dye removal using palm tree male flower activated carbon. Int J Appl Environ Sci 11(2):475–490

Taqui SN, Yahya R, Hassan A, Nayak N, Syed AA (2017) Development of sustainable dye adsorption system using nutraceutical industrial fennel seed spent-studies using congo red dye. Int J Phytoremediation 19(7):686–694

Taqui SN, Yahya R, Hassan A, Nayak N, Syed AA (2019) A novel sustainable design to develop polypropylene and unsaturated polyester resin polymer composites from waste of major polluting industries and investigation on their physicomechanical and wear properties. Polym Compos 40(3):1142–1157

Thejaswini TV, Prabhakaran D (2016) Synthesis of mesoporous titania–silica monolith composites —a comprehensive study on their photocatalytic degradation of acid blue 113 dye under UV light. Int J Nanosci 15(05n06):1660012–1660020

Toth J (1971) State equation of the solid-gas interface layers. Acta Chim Hung 69:311–328

Vidyashankar GK (2014) Fenugreek: An analysis from trade and commerce perspective. AJSIH

Vieth WR, Sladek KJ (1965) A model for diffusion in a glassy polymer. J Colloid Sci 20(9):1014–1033

Wang HL, Chen JL, Zhai ZC (2004) Study on thermodynamics and kinetics of adsorption of p-toluidine from aqueous solution by hypercrosslinked polymeric adsorbents. Environ Chem 23(2):188–192

Webber TW, Chakkravorti RK (1974) Pore and solid diffusion models for fixed-bed adsorbers. Alche J 20(2):228–238

Zaffalon (2010) Carbon mitigation and textiles. Textile World:35

Zayani G, Bousselmi L, Pichat P, Mhenni F, Ghrabi A (2008) Photocatalytic degradation of the acid blue 113 textile azo dye in aqueous suspensions of four commercialized TiO_2 samples. J Environ Sci Health A 43(2):202–209